Journal of Inorganic and Organometallic Polymers and Materials (2020) 30:613–621
https://doi.org/10.1007/s10904-019-01311-z

Influence of the Gamma Radiation on the Structure of PVDF/PANI Blend

A. S. El-Bayoumi[1]

Received: 17 January 2019 / Accepted: 3 September 2019 / Published online: 19 September 2019

Abstract
In this study, the gamma radiation altering effects on the structure and optical properties of Polyvinylidene fluoride (PVDF)/polyaniline (PANI) blend films was investigated. The PVDF and PANI films were synthesized by casting method and gamma irradiated at 50, 100, 125, and 150 kGy, respectively. Following the irradiation, the films morphology and optical properties were characterized by X-ray diffraction technique (XRD), Fourier Transform Infrared spectroscopy (FT-IR) and ultraviolet–visible (UV–Vis) spectrophotometer. The optical constants, absorbance X (λ) and complex dielectric constant were calculated by using Swanepole method whereas the optical dispersion parameters E_o and E_d were determined by Wemple–DiDmenico and the high frequency dielectric constant (ε_∞) was analyzed. XRD patterns revealed the partial crystalline nature of the films before and after irradiation. FT-IR spectral analysis showed a slight shift and increase in the transmittance for all films post-irradiation. In conclusion, irradiating the PVDF and PANI films altered their optical properties suggesting degradation of the polymeric chains upon irradiation and the formation of new cross links.

Keywords Gamma irradiation · X-ray diffraction technique (XRD) · Fourier transform infrared spectroscopy · Optical parameters · Dispersion parameters

1 Introduction

The polyvinylidene fluoride (PVDF) polymers are thermoplastic polymers which are known for their superior thermal and electrochemical stability and corrosion resistance properties. This made them the polymer of choice in the nonmetallic heat exchanger and piezoelectric-film sensor industries [1]. So, blends and composites with conventional polymers have received great attention since these new materials combine the excellent mechanical Properties and high process ability of the usual polymers with the electric conductivity of conducting polymers. New properties may originate from specific interaction between the material and the added amount of (PANI) in addition to the particular arrangement of the filler particles in the host matrix [2]. Moreover, optical and mechanical properties for irradiated polymers associated with their structure were investigated PANI (Polyaniline) ranks first among conducting polymers in research, due to easily synthesized chemically also electrochemically, doped easily and its particular electrical and optical properties. But the lowering of chemicals Obtained PANI is its weak soluble in organic solvents and weak fusibility, so it is ungovernable to be prepared as a cast film. So it is necessary to blended and composites with conventional polymers which is has great attention because off these new materials has excellent mechanical properties than the other polymers used. New Different features are observed in the UV–Vis optical absorbance spectra of electrochemically deposited PANI films at different pH. The evaluation introduces the versatility of application of these features for analytical purposes. Actually sensitivity of PANI films can be used in physiologically important pH interval [3]. Also, PVDF has been extensively examined for its electrical effects in general and the effect of its polymorphic construction used as aspects of the electronic advances PVDF are used in transformers, voltage sensors, and IR imaging [4]. PVDF compared with other materials, is known by its ease in application at low temperature, flexibility, and good electrical property [5]. PANI was blended with the PVDF

✉ A. S. El-Bayoumi
ahmed_shawki2007@yahoo.com

[1] Radiation Physics Department, National Center for Radiation Research and Technology (NCRRT), Atomic Energy Authority of Egypt (AEAE), Nasr City, Cairo, Egypt

polymer; hence the blend would enhance the thermal conductivity of the PVDF polymers and overcome the poor physical properties of the PANI polymer. However, the immiscible blend obtained changes in its electrical conductivity, according to the pH of the solution in which it was immersed, indicating the possibility of the real application of that material as a resistor with variable electrical resistance [6]. Also, X-ray diffraction measurements were used to investigate the effect of PANI on the structure and morphology of PANI/PVDF composites shows its semi crystalline nature [7, 8]. Using FTIR spectroscopy, it appeared that pure PANI polymer harbors a N–H stretching bond at about 3430 cm^{-1}, aromatic C–H stretching bond at 2920 cm^{-1}, benzenoid ring stretching bond at 1494 cm^{-1} and a quinoid ring stretching bond at 1483 to 1585 cm^{-1}. On the other hand, the spectra of the PVDF polymer showed a significant stretching peak at 840 cm^{-1} which indicates a β-phase and a peak at 1170 cm^{-1} for the C–F bond present in the polymer chain itself [9, 10]. One of the polymers of choice which upon blending with the PVDF enhance its thermal conductivity is PMMA. The PMMA/PVDF blends showed a strong shift in the absorption band which indicated intermolecular interaction between both polymers [11]. This in turns enhanced the desirable electrical and optical properties of PVDF [12]. To further enhance the optical and electrical properties of the blend, the blends were subjected to ionizing radiation. Irradiation by ionizing radiation has been found to induce changes in the chemical structure and physical properties of polymers. Such changes may be in the form of crosslinking, main chain session, or evolution of hydrogen depending upon the radiation X-ray diffraction after irradiated dose between 100 kGy at 3000 kGy increasing crystallinity for PVDF films with increasing irradiation dose, although the melting latent heat is decreasing [13]. The gamma radiation is a convenient and effective way of modification per fluorinated and partially fluorinated polymers such as PVDF. The properties of the pristine and irradiated PVDF at different doses (5, 10, 12.5 and 15 kGy) were studied by infrared spectroscopy suggesting that the radiation caused the crosslinking or chain scission of the PVDF film [14]. Moreover, optical and mechanical properties for irradiated polymers associated with their structure were investigated.

Upon gamma irradiation of the blended PVDF/PANI polymers, the physical properties of the blends were modified. The observed changes were highly dependent on the internal structure of the polymers, the applied radiation dose and the thickness of the samples. In this work we study the gamma radiation effect on pure PVDF and PVDF/PANI composite films, through remarking and measuring the change in the structure of the samples by using X-Ray diffraction, UV–Vis and FTIR spectrophotometer.

2 Experimental

2.1 Sample Preparation

The PVDF/PANI blend was prepared as plasticized free standing films using the co-dissolution method. Polyaniline, in the conducting emeraldine salt form, is obtained from Fluka (Germany). PVDF powder is obtained from International laboratory, USA (Mw = 534 000). 10 grams of PVDF were dissolved in 60 ml dimethylformamide (DMF) for 2 h at 40 °C and 0.1 g in 20 ml of (DMF) for 2 h at 40 °C. The dissolved PANI was added in a drop wise manner to the PVDF solution. The solution was stirred at 50 °C for 2 h, until obtaining viscous and homogenous blend. The blend were casted as films on glass substrates and left to dry at ambient atmosphere at 60 °C for several days to remove the solvent.

2.2 Characterizations and Techniques

All prepared films of thickness 0.009 cm were irradiated by Egypt's MEGA, gamma I, supplied as type J-6500 by the Atomic Energy of Canada Ltd with a ^{60}Co source at a dose rate of 9.23 kGy/h with accumulated dose from 50 up to 150 kGy. The irradiated films were characterized using a fully computerized X-ray diffractometer, Shimadzu XRD-6000 with Cu radiation λ = 1.54056 Å at National Center for Radiation Research and Technology, Egyptian Atomic Energy Authority. The X-ray tube was operated at 40 kV and 30 mA anode current throughout the measurements. The above operation conditions were maintained during all the relevant measurements. The 2θ scan range from 4° to 90° continuous scanning with scan speed 8°/min and preset time 0.15 s was used for the entire 2θ-range. The optical properties were measured over range 200–1200 nm using double-beam Jasco V-670 UV/VIS spectrophotometer. All optical and X-ray diffraction measurements were carried out before and after gamma irradiation. In addition, molecular vibration modes of bonds were generally characterized by FT-IR transmission or absorption bands as a function of wavenumber using a BRUKERVERTEX 70 v vacuum FT-IR spectrophotometer. All the measurements were done in the range of 400–4000 cm^{-1}.

3 Results and Discussion

3.1 XRD Diffraction and Structural Investigations

XRD diffraction was employed to examine the gamma radiation effect on the structure of the PVDF and PVDF/PANI

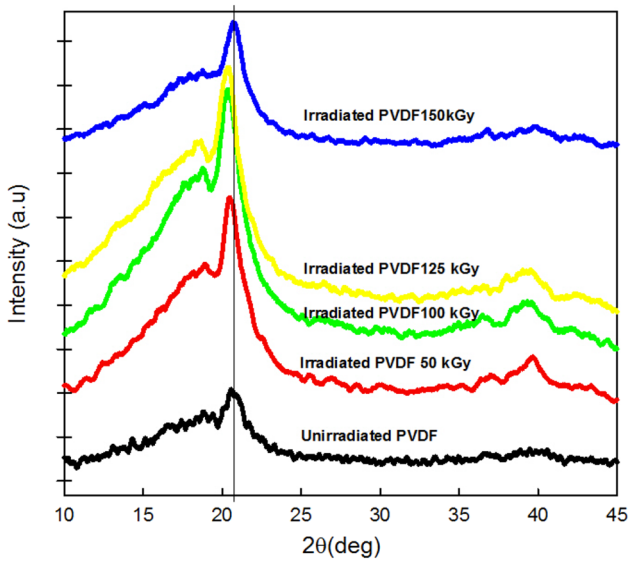

Fig. 1 XRD patterns of PVDF film for un-irradiated and irradiated doses

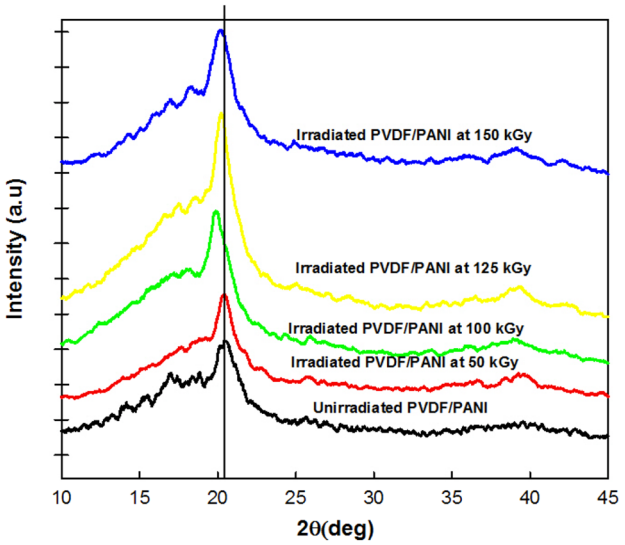

Fig. 2 XRD patterns for un-irradiated and irradiated PVDF/PANI blended films

films. It could be noted that gamma radiation affected the physicochemical properties of radiated films. Figure 1 shows the X-ray spectrum of the as-cast PVDF film. The spectrum indicated that the PVDF film is at the β-phase. All the broadened peaks corresponded to the β-phase. The XRD peaks of PVDF appears at 2θ value 27.4219°, with the peaks shifted and intensity increased post-irradiation up to 150 kGy. The considerable broadening in the XRD patterns post irradiation gave the indication of increased distortions. A continuous increase in the peaks intensity was observed in a dose dependent manner upon increasing the radiation dose from 50 to 150 kGy indicating a grain growth [15].

Figure 2 shows the structural changes observed in PVDF/PANI induced by gamma radiation as revealed by XRD. It is quite evident from that the main peak appearing at around 2θ ~ 20.25° corresponds to a d spacing of 4.54397 Å and a reflection plane of (200) to the host material PVDF. For all films, a major shift in the diffraction patterns with fluctuating peak intensity was observed in both un-irradiated and irradiated films upon only upon changing the radiation doses. The appearance of such intense and broad peak is probably attributed to the formation of strong intermolecular and intermolecular interactions between the polymer chains. [16].

In addition, XRD diffraction was employed to examine the impact of gamma radiation on some physical parameters of PVDF and PVDF/PANI Films. The XRD pattern for PVDF and PVDF/PANI films is approximately in agreement with ICDD data (card no. 42-1651) respectively. The crystal size (D) for PVDF and PVDF/PANI films with different ratio for un-irradiated and irradiated films is estimated using the Scherer's formula:

$$D = \frac{K\lambda}{\beta \cos\theta} \tag{1}$$

where λ, θ and β are the X-ray wavelength (1.54056 Å), Bragg diffraction angle and full width at half maximum of (β) diffraction peak, respectively. The strain (ε) was calculated using the relation

$$\varepsilon = \frac{\lambda}{D\cos\theta} - \frac{\beta}{\tan\theta} \tag{2}$$

The dislocation density (δ), which is defined as the length of dislocation lines per unit volume of the crystal, and distortion parameter or Lattice parameter was calculated from the relation

$$\delta = \frac{1}{D_{hkl}^2} \text{ and } g = \frac{\beta}{\tan\theta} \tag{3}$$

As shown in Table 1, increasing the radiation dose from 50 kGy up to 150 kGy decreases the crystal size which consequently increases the strain in the PVDF and PVDF/PANI films [17]. This resultant strain affected the mechanical properties of the crystal reducing the stability of its microstructure and adhesiveness of the films. Moreover, the XRD diffraction was employed to examine the impact of gamma radiation on increasing the strain, dislocation and distortion parameters which led to decrease in crystal size of the polymeric matrix. Reduction in the crystal size may decrease the mass transportation among neighboring particles during the crystal growth stage contributing to the formation of smaller grains indicating the degradation of the polymeric chains rather the formation of new crosslink [12].

Table 1 Crystal size, strain, dislocation density and distortion parameters of un-irradiated and irradiated PVDF and PVDF/PANI blended films

Films	PVDF				PVDF/PANI			
	D (nm)	Dislocation density ($\delta \times 10^{16}$)	Strain ($\varepsilon \times 10^{2}$)	Distortion (g)	D (nm)	Dislocation density ($\delta \times 10^{16}$)	Strain ($\varepsilon \times 10^{2}$)	Distortion (g)
Un-irradiated	5.984	2.79	1.451	1.306	5.313	3.54	1.649	1.485
Irradiated 50 kGy	5.609	3.18	1.559	1.404	5.148	3.77	1.668	1.501
Irradiated 100 kGy	5.384	3.45	1.629	1.467	4.809	4.32	1.798	1.619
Irradiated 125 kGy	5.143	3.78	1.712	1.541	4.669	4.59	1.871	1.684
Irradiated 150 kGy	4.946	4.09	1.769	1.592	4.54	4.85	1.891	1.702

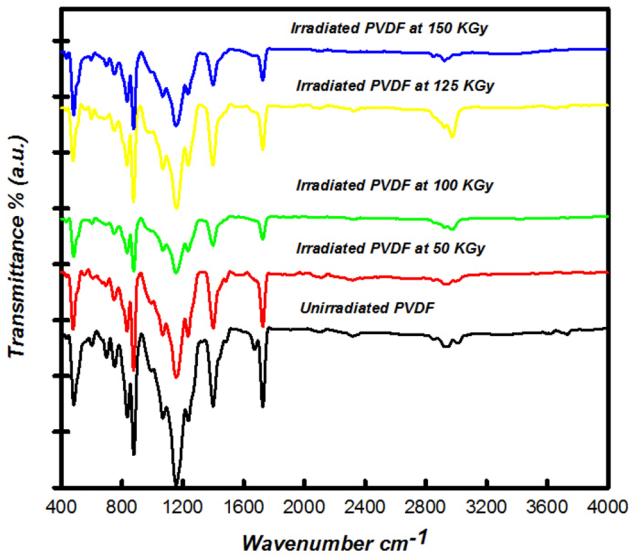

Fig. 3 FTIR spectra for un-irradiated and irradiated PVDF film

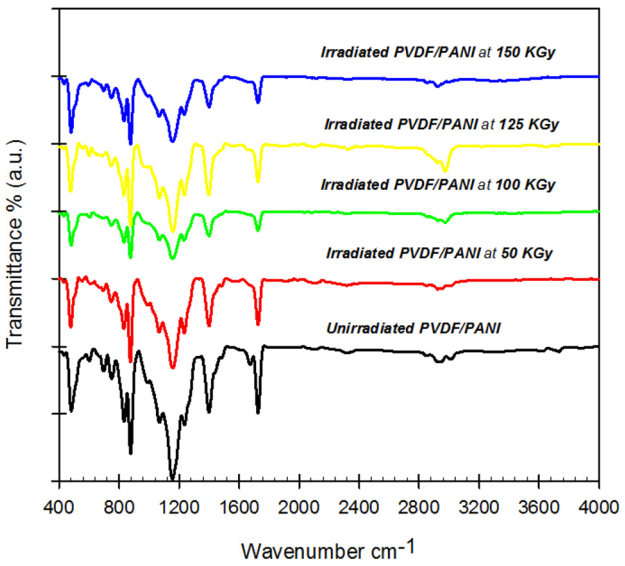

Fig. 4 FTIR spectra for un-irradiated and irradiated PVDF/PANI blended films

3.2 FT-IR Spectroscopic Analysis

The structural changes in the PVDF and PVDF/PANI polymers films induced by gamma radiation were inspected by infrared transmission FTIR spectroscopy. The FT-IR spectra of the non-irradiated and irradiated PVDF and PVDF/PANI blend was recorded between 3800 and 400 cm^{-1} at the radiation doses 0, 50, 100, 125 and 150 kGy as shown in Figs. 3 and 4. The main FTIR peaks for the PVDF/PANI blends as well as their assignments are recorded in Table 1.

Figure 3 shows the FT-IR spectra of pure PVDF before and after irradiation which are in coincidence with those reported previously. Spectra of pure PVDF indicates the presence of stretching vibration band located at 1400 cm^{-1}, 1234 cm^{-1}, 1157 cm^{-1} and 877 cm^{-1} which is characteristic to C–C vibrations, 834 cm^{-1} and 751 cm^{-1} to CH_2 rocking vibrations. Also, the band at 1069 cm^{-1} related to CF_2 bending [12, 18]. The broad band at 3482 cm^{-1} shifted to 3500 cm^{-1} is assigned to the O–H stretching vibration of the hydroxyl group of physically adsorbed water molecules. Two characteristic bands corresponding to asymmetric stretching vibration of (CH_2) and C–H were observed at 3013 cm^{-1} and 2958 cm^{-1}, respectively [18, 19]. After exposure to gamma radiation, increase in the intensity and broadness of hydroxyl groups was observed. As the radiation dose increased to 50 and 100 kGy, the PVDF characteristic band got sharpened and the intensity proceeded to increase at 1081, 1153 and 1243 cm^{-1} until the maximum was achieved at 100 kGy this indicated that the samples acquire amorphous nature (Table 2).

As shown in Fig. 4, the transition bands of the PVDF/PANI blend (10 wt% PANI) at 482 and 834 cm^{-1} indicated as β phase of the pure PVDF. Other transition bands appeared at 1235 and 1156 cm^{-1} in the same spectrum are related to the C–F stretch of the PVDF polymeric chain [20]. The PANI's characteristic bands include the N–H stretch at 3430 cm^{-1} and the aromatic C–H stretch at 2920 cm^{-1}

Table 2 Lists the main FTIR peaks of PVDF– PANI and their possible assignments

Wavenumber (cm^{-1})	Assignments
834	(CF_2) of PVDF
876	(C–C) and (CF_2) of PVDF
1071	(C–C) (CF_2) and (CH_2) of PVDF
1169	(CF_2) and (CH_2) of PVDF
1231	(CF2) and [(CH_2)] of PVDF
1404	(CH2) and (C–C) of PVDF
1494	stretch of benzene rings
1585	stretch frequency of quinone ring
1680	DMF solvent
2920	aromatic C–H stretch
3430	N–H stretch

[21, 22]. The benzene ring stretch of the PANI appeared at 1400 cm^{-1} while the quin one ring stretch occur at 1483 cm^{-1} [21, 22]. The band aroused at 1726 cm^{-1} is attributed to DMF solvent. It could be noted that the addition of PANI modifies the PVDF molecular structure. The sharpened peak at 1153 cm^{-1} is a characteristic feature of the PANI and its intensity increased upon increasing the radiation dose till 100 kGy then began to decrease gradually. This behavior indicated the dissociation of the PANI polymer into ions. Increasing the gamma radiation dose stimulates ionic dissociation which is reflected in the FTIR spectra as an increase in the intensity of the peaks. These results depicted from FTIR spectra of non-irradiated and irradiated samples as shown in Fig. 4 are particularly in good agreement with the results of XRD and UV/Vis studies .

3.3 Optical Parameters

3.3.1 Determination of Refractive Index

The refractive index and absorption coefficient were determined using both the transmission and reflection spectra. The complex refractive index (n′) for a film of thickness d was deduced by the formula ($n' = n + iK$), where n is the refractive index and K is the extinction coefficient. This was related to the absorption coefficient α through the relation: $\alpha = 4\pi K/\lambda$. The reflectivity of an absorbing medium that incidence n and K in air for normal incidence is given by [23]

$$n = \left(\frac{4R}{(1-R)^2} - K^2\right)^{1/2} + \left(\frac{1+R}{1-R}\right) \quad (4)$$

Figure 5 conveyed the relation between the refractive index (n) against the incident wavelength range 200–1500 nm. Notably, the refractive index decreased upon increasing wavelength of the incident photon. However, at higher wavelengths, the refractive index tended to be constant. This phenomenon might be attributed to the polymer cross linkages induced by gamma

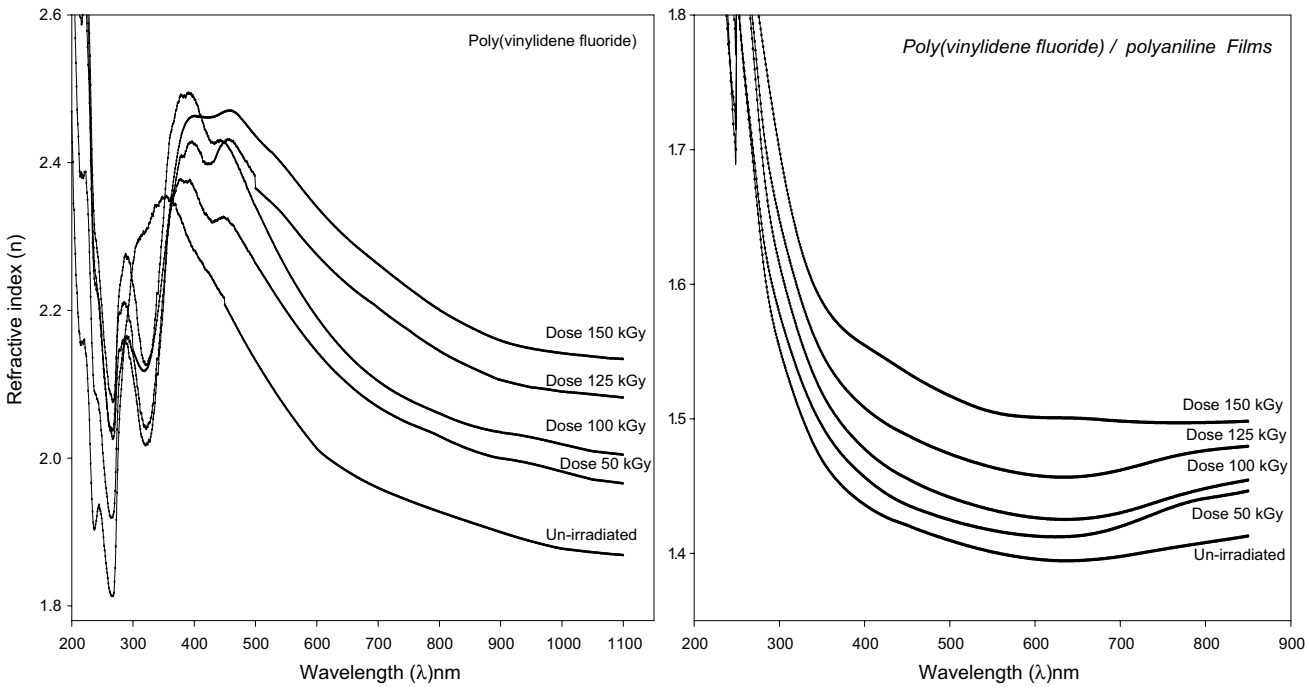

Fig. 5 the relation between the refractive index (n) against the incident wavelength. For **a** pristine PVDF and **b** PVDF/PANI blend with different dose

radiation and the formation of new covalent bonds [23]. The polymer cross linkage hinders the motion of molecules and reduce its activities which in turn decrease the refractive index. Furthermore, the polymer structure is assumed to be Pesudo-crystalline and the crystallinity increased upon increasing the irradiation dose. At higher dose (150 kGy), the chains scission became predominant relative to the polymer crosslinking. The irradiation dose was further increased from 50 to 150 kGy to stimulate various degrees of crosslinking. Thus, the refractive index of PVDF decreases evidently as the irradiation dose increases to 50 kGy and it reached its lowest value at the radiation dose 100 kGy as shown in Fig. 5.

3.3.2 Dispersion Parameters

Generally, the single oscillator parameter E_o (the single oscillator energy) and E_d (dispersive energy) for the films have been calculated and discussed in terms of the Wemple–DiDmenico model. The oscillator energy E_o is, to a fair approximation, related empirically to the lowest refractive index [24, 25]. These parameters are calculated by using the equation

$$n^2(E) = 1 + \left[\frac{E_0 E_d}{E_0^2 - E^2}\right] \tag{5}$$

By plotting $(n^2-1)^{-1}$ versus E^2 (photon energy)^2, a straight line is obtained as shown in Fig. 6a, b, E_o and E_d are determined directly from the gradient, $(E_o\, E_d)^{-1}$ and the intercept (E_o/E_d), on the vertical axis. On the other hand, the parameters E_o and E_d are then given by;

$$E_0^2 = \frac{M_{-1}}{M_{-3}} \text{ and } E_d^2 = \frac{M_{-1}^3}{M_d} \tag{6}$$

Since the M_{-1} and M_{-3} moments which are involved in computation of E_o and E_d. The dispersion energy may depend upon the detailed charge distribution within each unit cell, consequently, would then be closely related to chemical bonding that may lie within a nearly orbital theory. On the basis of the above mentioned model, the single–oscillator parameter increases from $E_o \approx 3.854$ for PVDF to 6.305 for PVDF/PANI composite. It is also noted that E_d decreases from ≈ 6.838 eV for PVDF films to 2.009 eV for PVDF/PANI composite. On the contrary, E_d increases upon increasing the irradiation doses for both films as listed in Table 3.

The irradiation doses altered the optical constants of all films. At long wavelengths, a positive deviation from linearity was noticed and attributed to the negative effect of the lattice vibrations to the refractive index. On the contrary, at short wavelength, a negative deviation to the proximity of band edge or exitonic absorption was noted. The refractive index was analyzed to determine the long-wavelength refractive index n_∞, average oscillator wavelength λ_0 and oscillator length strength S_0 of the films. In order to determine these parameters, the single-term Sellmeier oscillator was used [26]

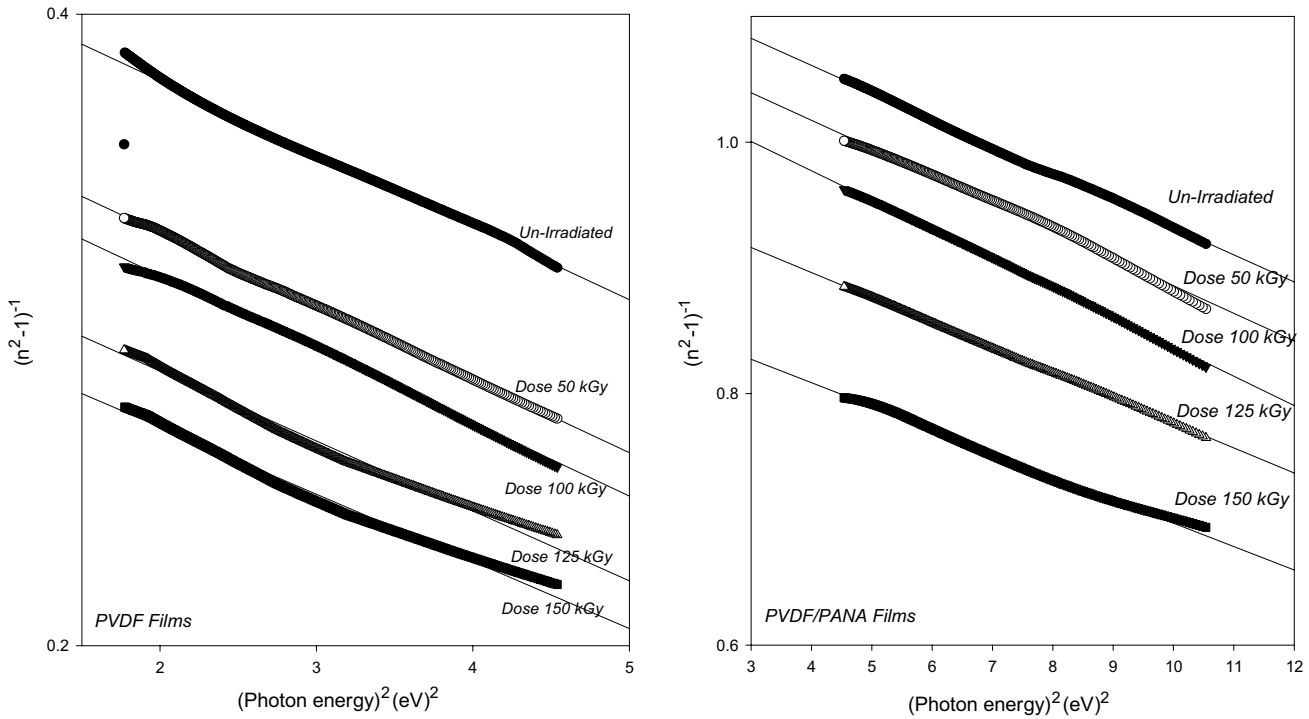

Fig. 6 shows plotting of straight lines fitted for $(n^2-1)^{-1}$ versus E^2 for **a** pristine PVDF and **b** PVDF/PANI blend with different dose

Table 3 Optical Dispersion parameters for PVDF and PVDF/PANI films before and after Gamma irradiation with different doses

	PVDF				PVDF/PANI			
	E_o	E_d	M_{-1}	M_{-3}	E_o	E_d	M_{-1}	M_{-3}
Un-irradiated	3.854	6.838	1.774	0.121	6.305	2.009	0.319	0.008
Dose 50 kGy	3.702	7.478	2.019	0.147	6.285	2.161	0.344	0.009
Dose 100 kGy	3.685	8.001	2.171	0.159	6.214	2.37	0.382	0.011
Dose 150 kGy	3.649	8.391	2.299	0.173	5.998	2.906	0.485	0.013

$$\frac{n_\infty^2 - 1}{n^2 - 1} = 1 - \left(\frac{\lambda_0}{\lambda}\right)^2 \tag{7}$$

This method describes the contribution of the free carrier and lattice vibration modes of the dispersion [28] and extrapolation of the linear part of the curve in this figure to zero wavelength gives the values of $n^2 = \varepsilon_\infty$. In the low absorption region, the refractive index n can be expressed by the single oscillator model [27]. Given from the relation

$$n^2 - 1 = S_0\left(\frac{\lambda_0^2}{1 - \left(\lambda_0/\lambda\right)^2}\right) \tag{8}$$

where λ_0 is an average inters band oscillator position and S_0 is the average inters band oscillator strength. Figure 7 shows the plot of $1/(n^2-1)$ versus $1/\lambda^2$ which is a straight line in accordance with the previous equation. The evaluated values of S_0 and λ_0 films are shown in Table 3 for un-irradiated and irradiated films for both PVDF and PVDF/PANI, respectively. As a change of gamma radiation doses, the chain scission becomes predominant relative to the crosslinking which modifies the molecular structure and hinders the growth of crystal [12].

3.3.3 Complex Dielectric Constant

In addition, assuming that the frequency is relatively high since the present reflectively measurements were performed in the Ultraviolet range and near—infrared spectral region. The dielectric constant could be calculated using the dispersion relation of the incident photon. The fundamental electron excitation spectrum of a substance is generally described in terms of a frequency—dependent complex electronic dielectric constant ε (ω)

$$\varepsilon(\omega) = \varepsilon_1(\omega) + i\varepsilon_2(\omega) \tag{9}$$

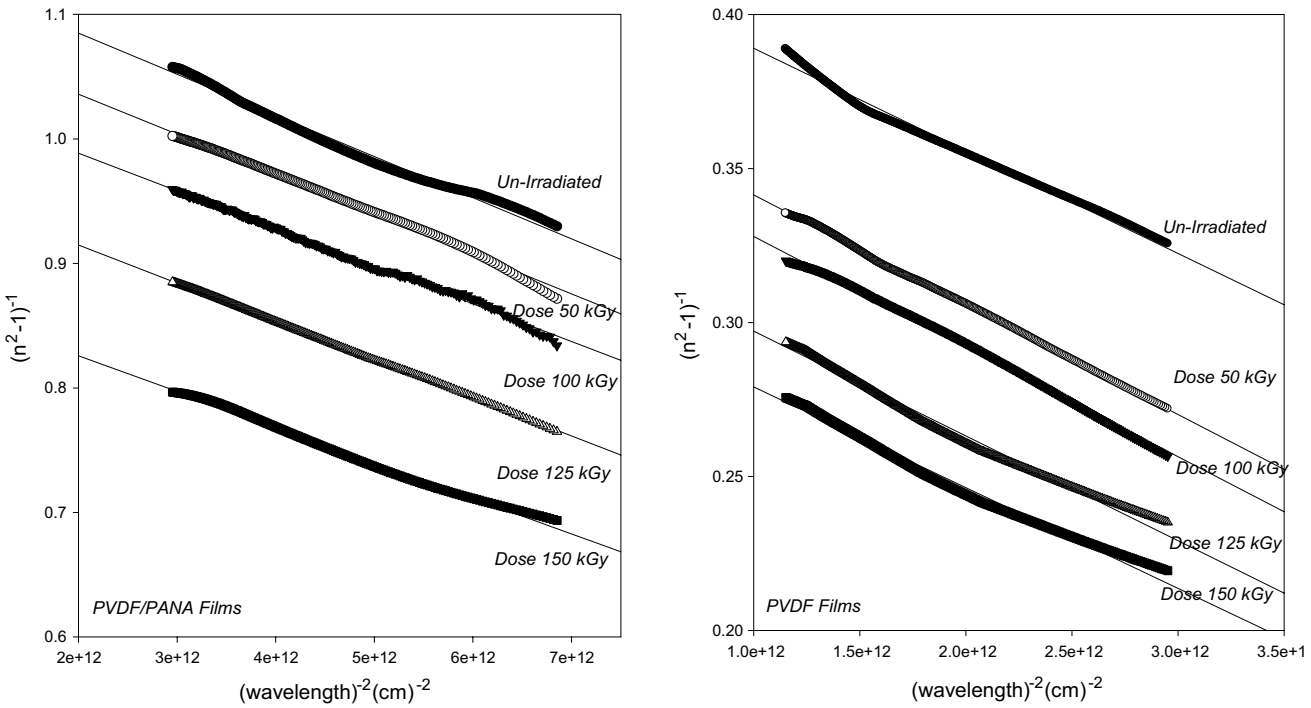

Fig. 7 Shows the plot of $1/(n^2-1)$ versus $1/\lambda^2$ for **a** pristine PVDF and **b** PVDF/PANI blend with different dose

Table 4 Optical parameters for PVDF and PVDF/PANI films before and after gamma irradiation with different doses

Samples	PVDF			PVDF/PANI		
	ε_∞	ω_P (10^{11}/s)	N/m* (10^{28}/cm^3)	ε_∞	ω_P (10^{11}/s)	N/m* (10^{27}/cm^3)
Un-irradiated	2.586	1.608	2.605	1.313	5.903	1.782
Dose 50 kGy	2.917	1.725	3. 383	1.351	5.994	1.891
Dose 100 kGy	3.022	1.887	4.195	1.374	6.385	2.182
Dose 150 kGy	3.121	1.998	4.855	1.485	6.961	2.804

Either the real part $\varepsilon_1(\omega)$ or the imaginary part $\varepsilon_2(\omega)$ contains all desired response information. The real ε_1 and imaginary ε_2 parts of the complex dielectric constant can be written as the following relations [28].

$$\varepsilon_1 = n^2 - K^2 = \varepsilon_\infty - \frac{e^2}{4\pi^2 C^2 \varepsilon_0}\frac{N}{m^*}\lambda^2 \tag{10}$$

And

$$\varepsilon_2 = 2nK = \frac{\varepsilon_\infty \omega_p^2}{8\pi^2 C^3 \tau}\lambda^3 \tag{11}$$

Where

$$\omega_p = \left[\frac{e^2 N}{\varepsilon_0 \varepsilon_\infty m^*}\right]^{1/2} \tag{12}$$

where ω_P is the plasma resonance frequency for one kind of free carriers, $\varepsilon_\infty$the high frequency dielectric constant, e the electronic charge, C the velocity of light, ε_o the free space dielectric constant, N/m* the ratio of free carrier concentration (N) to the free carrier effective mass(m*) and τ is the optical relaxation time. Where, the shift in the plasma edge towards a higher frequency could be attributed to the relatively high value of the carrier concentration. The ionic dispersion is normally referred to the lattice dispersion induces intense absorption at the short wavelength side of the main absorption edge while, the long wavelengths absorption is usually attributed to the free carrier. Equations (10) and (11) were employed to determine the parameters, ε_∞, ω_p and N/m*. The values of, ε_∞, ω_p and N/m* are listed in Table 4.

4 Conclusions

From the above discussion, we can be conclude that:

1. The XRD diffraction spectral analysis of all films confirmed that the amorphicity of the films was reduced with a slight decrease in the crystallized particles upon irradiating the films at 50, 100, 125, and 150 kGy, respectively. This change in the amorphicity was associated with improvement in the mechanical property and stability of the films.
2. It is evident from FT-IR spectral analysis that most types of CF2 and CH2 group frequencies observed in both the un-irradiated as well as the irradiated PVDF and PVDF/PANA which agreement with the previous studies.
3. Altering the radiation dose affected the refractive index of PVDF and PVDF/PANA films. The refractive index dispersion parameters E_0 and E_d decreased upon increasing the radiation dose up to 150 kGy which was adequately described by the single oscillator model. The high frequency dielectric constant (ε_∞) and N/m* were as well affected following the irradiation of the films, they were found to be decreased by irradiation. The value of S_0 and n_0 were calculated for both un-irradiated and irradiated films.

References

1. H. Guo et al., Chin. J. Chem. Eng. **26**(5), 1213 (2018)
2. G. Kaur et al., RSC Adv. **5**(47), 37553 (2015)
3. M. Gicevicius et al., J. Electrochem. Soc. **165**(14), H903 (2018)
4. X. Cai et al., RSC Adv. **7**(25), 15382 (2017)
5. L. Ruan et al., Polymers **10**(3), 228 (2018)
6. E.A. Sousa et al., Polym. Bull. **74**(5), 1483 (2017)
7. S. Saïdi et al., J. Phys. D **46**(35), 3551 (2013)
8. S. Saïdi et al., Mater. Sci. Semicond. Process. **19**, 130 (2014)
9. S.M. Pawde, D. Kalim, J. Appl. Polym. Sci. **114**(4), 2169 (2009)
10. G.W. Duarte et al., Matéria **22**(3), 0193 (2017). https://doi.org/10.1590/s1517-707620170003
11. L.F. Malmonge et al., Eur. Polym. J. **42**(11), 3113 (2006)
12. A.S.M. Batista, C. Pereira, L.O. Faria, World Acad. Sci. Eng. Technol. Int. J. Chem. Mol. Nucl. Mater. Metall. Eng. **10**(2), 148 (2016)
13. G. Ribeiro, et al., International Nuclear Atlantic Conference—INAC 2009
14. L. Shen et al., Sci. Rep. **7**(1), 2721 (2017)
15. Q. Wang et al., Polym. Bull. **66**(6), 821 (2011)
16. L.Y. Tian, X.B. Huang, X.Z. Tang, J. Appl. Polym. Sci. **92**(6), 3839 (2004)
17. R. Hasegawa et al., Polym. J. **3**(5), 600 (1972)
18. Y. Peng, P. Wu, Polymers **45**(15), 5295 (2004)
19. B. Ahmad et al., Prog. Nanotechnol. Nanomater. **2**, 42 (2013)
20. P. Wang et al., Chem. Eng. J. **162**(3), 1050 (2010)
21. V. Aravindan, P. Vickraman, T.P. Kumar, J. Non-Cryst. Solids **354**(9), 3451 (2008)
22. R. Gregorio, N.C.P. de Souza Nociti, J. Phys. D **28**(2), 432 (1995)

23. S. El-Sayed et al., Physica B **464**, 17 (2015)
24. G. Ribeiro, et al., Gamma irradiation effects on poly (vinylidene fluoride) films. International Nuclear Atlantic Conference, Rio de Janeiro, RJ, Brazil. ISBN: 978-85-99141-03-8 (2009)
25. S. Wemple, M. DiDomenico, Phys. Rev. B **3**(4), 1338 (1971)
26. B. Zheng et al., Vacuum **85**(9), 861 (2011)
27. R. Bhunia, et al., Adv. Polym. Technol. (2016)
28. W. Sellmeier, Subst. Ann. Phys. Chem. **219**, 272 (1871)